JOURNAL OF CATALYSIS 69, 359–370 (1981)

The Surface Chemistry of Some Perovskite Oxides

MICHEL CRESPIN[1] AND W. KEITH HALL[2]

Department of Chemistry, Laboratory for Surface Studies, University of Wisconsin, Milwaukee, Wisconsin 53201

Received September 29, 1980; revised January 16, 1981

The surface hydroxyl concentrations of $BaTiO_3$, $SrTiO_3$, and $LaCoO_3$ were determined by exchange with D_2 as a function of the dehydroxylation temperature. The results suggest that the surface chemistry of these materials resembles that of certain other oxide systems such as alumina and titania. Values approaching the number of hydroxyls required to terminate the lattice ($1.4 \times 10^{15}/cm^2$) were obtained for samples evacuated at room temperature, but these values fell by about an order of magnitude as the pretreatment temperature was increased to 450°C and by another factor of about 2 at 600°C. In this way coordinatively unsaturated centers were produced. The experimental procedure was complicated somewhat by the fact that all three oxides were reduced to a greater or lesser extent when contacted with D_2 at elevated temperatures. This amount was negligibly small at 450°C (the temperature required for equilibration) with $BaTiO_3$ and $SrTiO_3$ but it amounted to about $1\,e$/mole for $LaCoO_3$ (e = electrons). The former two oxides could be reduced by about $0.4\,e$/mole at 1200°C. In all cases an amount of H_2O equivalent to that of the H_2 consumed was produced in the reduction step and the oxygen removed could be readily replaced on contact with O_2 at the same temperature. $LaCoO_3$ could be reduced by up to $3\,e$/mole at 500°C and the oxygen again replaced stoichiometrically. X-Ray patterns of the parent perovskites were in good agreement with literature values. The pattern for $LaCoO_3$ changed slightly when it was reduced by $1\,e$/mole, but returned to that of the parent sample on reoxidation at 450°C. The pattern of La_2O_3 appeared when the sample was reduced by $3\,e$/mole, but it again became nearly identical with that of the parent perovskite upon reoxidation. Lines for metallic Co did not appear at 500°C but became evident when the reduced sample was sintered in He at 800°C. In the latter case the perovskite lines returned only very slowly as Co_3O_4 reacted with La_2O_3 at this temperature. The catalytic implications of these observations are briefly discussed.

INTRODUCTION

The perovskites have long been of interest to solid-state chemists and physicists because of their technologically important physical characteristics such as ferroelectricity, piezoelectricity, pyroelectricity, magnetism, high-temperature superconductivity, and electro-optic effects. These isomorphic oxides have the general formula ABO_3, where A is usually a large ion with a filled d shell and B is a smaller transition metal ion. Ideally, the crystal structure is based on a cubic unit cell (Fig. 1) but tetragonal or rhombohedral distortions are not uncommon and these features are reflected in the X-ray patterns. Interestingly, small changes in structure and composition may result in large changes in electronic properties. The isostructural ABO_3 compounds include a wide variety of transition metal ions and vary from insulators and wide band-gap intrinsic semiconductors to metallic conductors and Mott insulators. The literature contains a wealth of information on the solid-state properties, which has been adequately covered in recent reviews (Refs. (*1–5*)).

The ready availability of a family of isomorphic solids with controllable physical properties makes the perovskites attractive for basic research in catalysis. So far such interest has centered around their redox chemistry and semiconducting properties (*1, 4*) and, more recently, around their uses

[1] On leave from the CNRS Institute for Solides a Organisation Cristalline Imparfaite, Orleans, France.

[2] To whom all correspondence should be addressed.

0021-9517/81/060359-12$02.00/0

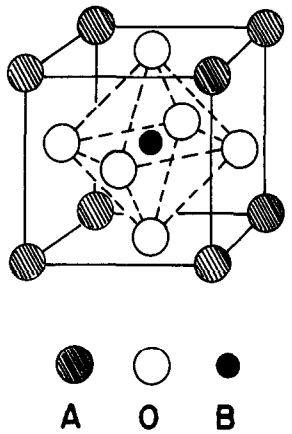

FIG. 1. Model of ideal perovskite crystal structure.

as photocatalysts and photoelectrodes for water splitting (*6–9*).

The perovskite structure is amenable to theoretical calculation of band structure and properties (*10–12*). These considerations have led to attempts to relate these results to chemisorption and catalysis. Such calculations usually either ignore surface states or are "cluster calculations" based on an assumed model of the surface. It seemed to us, therefore, that a study of the surface chemistry of these materials might be timely.

It is by now well known that the surfaces of most oxides are covered, to a greater or lesser extent, by a layer of hydroxyl groups. In principle, these should appear at all points where the surface oxygens would be coordinated to cations in the next highest layer, were they present. In practice, lower and lower values of surface OH concentration are frequently found as the pretreatment temperature in vacuum or dry gas is increased. These result from dehydroxylation processes as H_2O is formed by condensation. In this way coordinatively unsaturated cationic sites which may be of catalytic importance are developed as anion vacancies are introduced into the surface layers. Such information should be helpful in modeling the surface for theoretical work.

Three perovskites were selected for our study: $SrTiO_3$, $BaTiO_3$, and $LaCoO_3$. The first two were of the insulator–semiconductor band-gap type; the last is thought to have localized *d* orbitals (*1*). $BaTiO_3$ differs from $SrTiO_3$ by becoming ferroelectric below about 120°C, where the structure changes from cubic to tetragonal as the temperature is lowered through this region. This ferroelectric polarization is sufficient to produce substantial catalytic effects (*9, 13, 14*).

EXPERIMENTAL

Preparation of perovskites. To obtain samples of acceptable surface area, the method of Voorhoeve *et al.* was used (*15*). This involved precipitation of the metal ions A and B with a strong organic base from an equimolar solution of their nitrates in water. When cation B was Ti^{+4}, however, the nitrate was replaced by $TiCl_4$ dissolved in cold water at about 5°C. The base used was $(C_2H_5)_4NOH$, tetraethylammonium hydroxide (TEA), in excess of three times the stoichiometrically required amount; it was rapidly added to the stirred solution of the nitrates. The precipitate was washed with H_2O and separated by centrifugation repeatedly until the water came to a pH of 7.0. Finally, the precipitates were dried by evacuation for 48 h before being placed under flowing oxygen at the temperature used for calcination; this was determined by increasing the temperature in steps until only the X-ray pattern of the perovskite phase remained. The temperatures required were 550°C for $SrTiO_3$, 650°C for $BaTiO_3$, and 800°C for $LaCoO_3$ when the samples were treated for 10–15 h. Milder treatments which have sometimes been used (*16*) did not accomplish complete crystallization: The lines for the separated oxide phases remained evident.

Because preparations made in Pt (*17, 18*) have been shown to have catalytic activity due to Pt, only Pyrex or porcelain vessels were used in the present work. Moreover, TEA was substituted for KOH [which had been used previously (*14*) in the precipita-

tion step] to minimize contamination by alkali metals. Table 1 contains analytical data for impurities in our preparations that could have originated from Pyrex in contact with the strongly basic solutions.

Materials. Merck analytical reagent grade chemicals were used for these preparations. The organic base contained 20% TEA in distilled deionized water. The purity of $TiCl_4$ was >99.97%. The impurities (0.03%) which originated from the degradation of $TiCl_4$ were mainly chlorides and oxides of titanium (*19*). The specified metallic impurities contained in these reagents are listed in Table 2.

X-Ray characterization. The perovskite preparations were first examined by X-ray diffraction with a General Electric reflection diffractometer (Model No. XRD-5) using Cu$K\alpha$ radiation with a Ni filter placed between the sample and the detector to absorb a large fraction of the fluorescent rays originating from Co and La. Fe$K\alpha$ with a Mn filter was used in later experiments where the reduction of the $LaCoO_3$ was studied (to improve the sensitivity to Co).

Characterization of the surface. Surface areas were determined by the BET technique; the cross-sectional area of N_2 was taken to be 16.2 Å^2. The full isotherms were of Type II according to the Brunauer classification (*20*). The surface areas of the samples were 18, 16, and 64 m^2/g for $BaTiO_3$, $LaCoO_3$, and $SrTiO_3$, respectively. The larger surface area for $SrTiO_3$ probably resulted from the lower temperature required for its preparation.

The total hydrogen content of the perovskites was measured by exchange with D_2 using a method developed by Hall and co-workers (*21–23*). The BET system was modified for these measurements. A measured amount of D_2 was circulated over the sample in an all-glass loop by a magnetically activated pump; the hydrogen initially present in the solid was determined by the isotope dilution of the gas phase (H_2, HD, D_2). This isotopic exchange between the sample and the gas phase reached equilibrium rapidly at 450°C; raising the temperature further did not further change its composition.

A problem occurs with this technique when the solid is reducible, as with $LaCoO_3$. Two reactions occur simultaneously: reduction and exchange. In such cases it is necessary to be sure that the isotopic distribution in the water formed is the same as in the other two phases. We have shown previously (*23*) that this equilibrium could be reached by circulation of the gas phase (including the water) over a sample of molybdena on alumina heated to 450°C. In the present work, the reduction of

TABLE 2

Analysis of Reagents (ppm)

	$Ba(NO_3)_2$	$Co(NO_3)_2$	$La(NO_3)_3$	$Sr(NO_3)_2$
Ba	—	—	—	100
Ca	1000	—	—	50
Ce	—	—	300	—
Cu	—	10	—	2
Fe	2	10	—	5
K	—	—	—	50
Mg	—	—	—	50
Mn	—	50	—	—
Na	—	—	—	50
Nd	—	—	200	—
Sr	1000	—	—	—
Zn	—	50	—	2
Heavy as Pb	5	10	20	2

TABLE 1

Analysis for Selected Impurities in Perovskite Preparations (ppm)

Perovskite	Na^+	Cl^-	SiO_2	B
$BaTiO_3$	100 ± 10%	<10 ± 10%	10 ± 10%	500 ± 10%
$LaCoO_3$	100 ± 10%	50 ± 10%	100 ± 10%	12 ± 10%
$SrTiO_3$	100 ± 10%	20 ± 10%	<10 ± 10%	500 ± 10%

$LaCoO_3$ rapidly reached a plateau with time at 450°C; vide infra. Consequently, the equilibrium of the total gas phase occurred easily. This was established by the introduction of measured amounts of H_2O and determining the increase in hydrogen content associated with the exchange.

Cross-checks were made among analyses made by thermal conductivity, by mass spectrometry, and by chromatography. The maximum error for the amount of hydrogen present on the sample as quoted herein is estimated to be ±5%. The water obtained after reduction was measured back into the BET system with an overall accuracy of better than 5%. The extents of reduction (e/mole) were calculated from the equivalents of hydrogen consumed per equivalent weight of catalyst. The accuracy of these figures was better than 1%. Virtually all of this hydrogen appeared as water in the reduction step; vide infra.

Purification of gases. D_2 was purified before use by passage through a Pd thimble heated to around 350°C; H_2 and He were first passed over anhydrous $Mg(ClO_4)_2$ and then through a trap of high area active carbon cooled to −196°C; O_2 was purified by double distillation after passage over $Mg(ClO_4)_2$.

RESULTS

X-Ray Diffraction

The curves obtained for the different preparations, I vs. 2θ, are shown in Fig. 2. The patterns differed somewhat from one another as expected for the varying lattice parameters, but the peak indices corresponded to those published for the different perovskites (*24*, *25*). This permitted us to conclude that our preparations were mainly single phases as expected (*18*) when stoichiometric amounts of A and B are used in

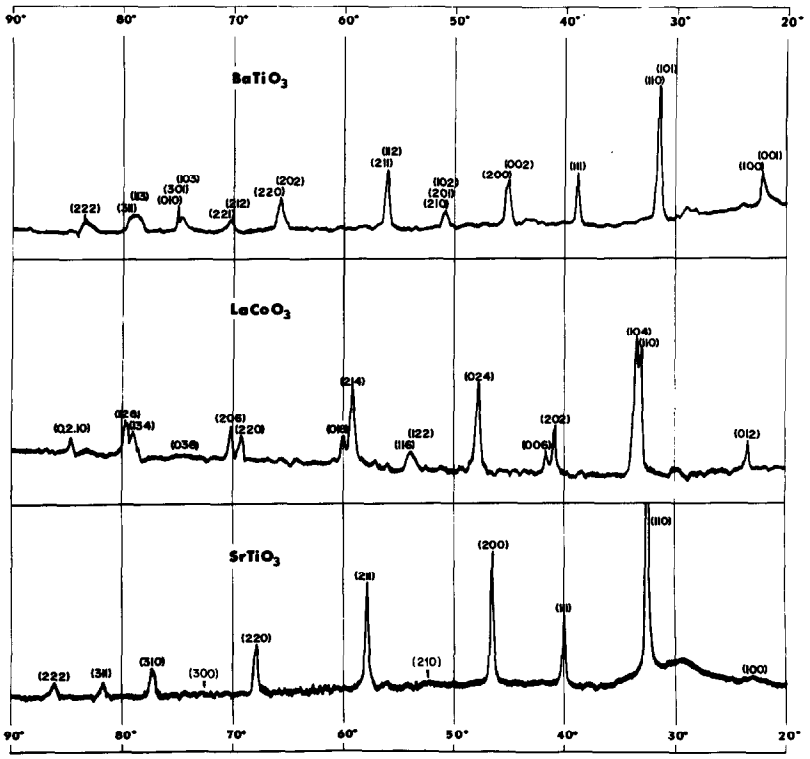

FIG. 2. X-Ray powder patterns of perovskite preparations studied. (The rhombohedral structure of $LaCoO_3$ is indexed with an hexagonal cell.)

the synthesis. With $LaCoO_3$, however, this result was obtained only at relatively high calcination temperatures (up to 800°C). At 700°C this preparation still contained more than 20% of a mixture of the very fine oxides (broad peaks). The fact that these perovskites form by diffusion of the oxides into each other at temperatures far below the melting point suggest that vacancies must be present in the lattice which could be of critical importance to catalytic action. The weak unindexed peaks at about 30°C may have stemmed from the glass support.

Determination of the Hydroxyls as a Function of Temperature

To eliminate all traces of organic residue, the samples were treated for 12 h at 500°C in flowing dry oxygen, followed by evacuation at the same temperature for 2 h. They were then cooled to room temperature and exposed to an equilibrium vapor pressure of water for 6 h. Finally, they were evacuated for 4 h at this temperature. The pretreated samples were heated in circulating He in steps from room temperature to 600°C. These temperatures were approximately 85, 205, 325, 450, and 600°C. Circulation time at each temperature was 2 h. In this way, H_2O produced by thermal dehydroxylation was collected in a liquid nitrogen trap. Finally, the system was evacuated through the trap for 90 min. The water of dehydroxylation was measured for each temperature. After reaching 600°C, the hydrogen remaining associated with the solid was determined by exchange with D_2 at 450°C as described above. Thus, by combining data and knowing the surface area of the sample, we could calculate the hydroxyl concentrations present at different temperatures. These results are shown in Table 3. Note that under these conditions only $LaCoO_3$ was reduced appreciably.

Reduction–Reoxidation in Relation to Structure

At 700°C, $SrTiO_3$ was reduced only to e/mole = 0.02. Data for reduction of $SrTiO_3$ and $BaTiO_3$ at 1200°C are presented in Fig. 3. At this temperature the extent of reduction, e/mole, remained less than 0.5 after 6 h. The color of these perovskites, which had been white in the oxidized state (yellow at high temperatures), darkened during reduction from sky blue (at 450°C) to a very dark blue as the reduction was increased. As judged by both color and X-ray patterns, these reduced samples appeared to be stable in air. The X-ray patterns (Fig. 2) remained virtually unchanged by these treatments, even though about one in 15 to 20 oxygen atoms was removed during reduction at 1200°C. Upon reoxidation at 600°C, however, the white color returned as the stoichiometry was restored.

The reduction–reoxidation data for all three perovskites are collected in Table 4. Within experimental error, the reactions were reversible, and stoichiometric. Moreover, virtually all of the water was produced in the reduction step. Note also the

TABLE 3

Surface Hydroxyl Concentrations of Selected Perovskites[a]

Composition	Surface area (m^2/g)	Pretreatment Temp.				
		25°C	150°C	300°C	450°C	600°C
$BaTiO_3$	18	13.8	5.9	2.8	1.5	0.55
$LaCoO_3$	16	11.9	9.4	5.0	1.2	0.65
$SrTiO_3$	64	8.3	3.9	1.5	0.5	0.30

[a] Calculated as OH × $10^{-14}/cm^2$. For full surface coverage, we calculated: $OH/cm^2 \simeq 14 \times 10^{14}$ for ⟨[(100) + (110) + (111)]/3⟩.

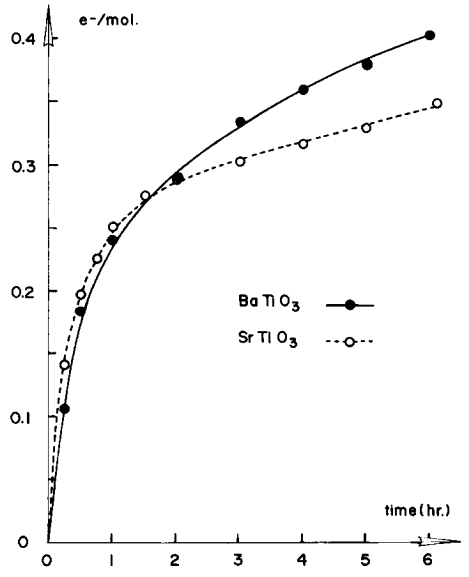

FIG. 3. Reduction of $BaTiO_3$ and $SrTiO_3$ in H_2 at 1200°C.

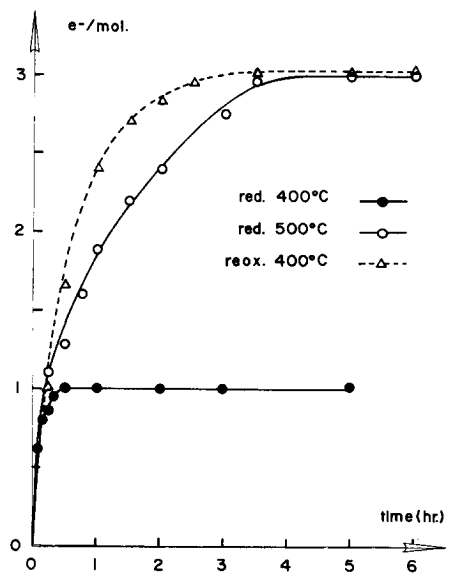

FIG. 4. Reduction and reoxidation of $LaCoO_3$ in H_2 and O_2 at indicated temperatures.

fair agreement between the H_2 consumed for reduction and the oxygen atoms ($2 \times O_2$ consumed) required for reoxidation.

$LaCoO_3$ was much more easily reducible. At 500°C, half of the oxygen could be removed in a few hours (Fig. 4). Reoxidation was stoichiometric and even more rapid. At 400°C, the reduction did not exceed 1 e/mole. The data of Fig. 4 and Table 4 suggest that the reduction of this material occurred in two stages, and this was further explored in the following experiment. D_2 was circulated over $LaCoO_3$ as the temperature was raised continuously from room temperature to 700°C at about 3°C/min, with water being removed as formed by the liquid N_2 trap. Changes in pressure, corresponding to consumption of D_2, were recorded and from these, Fig. 5 was derived. In separate experiments, these results were duplicated to the various stages indicated by small letters on Fig. 5. (Points c and f are for samples b and e, respectively, after reoxidation.) These symbols also represent the X-ray patterns taken at the end of these experiments which are shown in Figs. 6a–f.

TABLE 4

Reduction and Reoxidation of Perovskites[a]

Perovskite	Reduction temp. (°C)	Extent of reduction (e^-/mole)	Gas consumed or produced (cm^3(NTP)/g)			
			During reduction		During reoxidation	
			H_2	H_2O	$2 \times O_2$	H_2O
$BaTiO_3$	1200	0.40	19.34	18.46	19.76	0.04
$SrTiO_3$	1200	0.37	22.54	22.04	22.72	0.27
$LaCoO_3$	400	1.01	46.20	43.92	47.24	—
$LaCoO_3$	500	3.00	136.70	129.56	137.66	0.23

[a] Reoxidation was carried out in the recirculation system at 600°C with $BaTiO_3$ and $SrTiO_3$ and at 400°C with $LaCoO_3$ ation system.

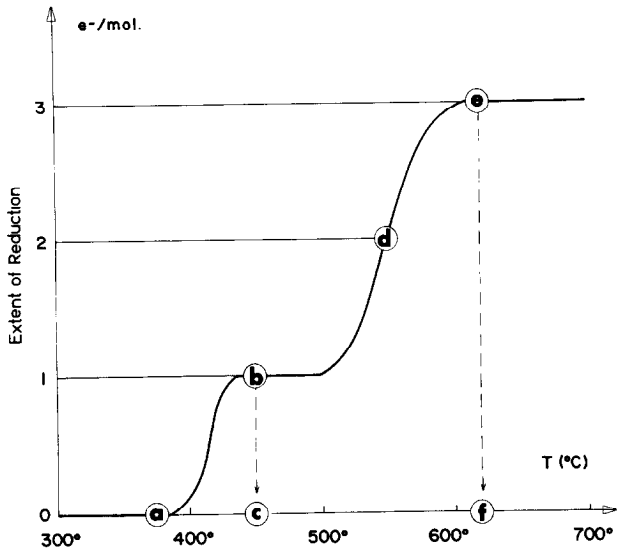

FIG. 5. Temperature-programmed reduction of $LaCoO_3$. Samples were prepared for X-ray examination in separate experiments terminated at the points indicated by the circled labels. Points (c) and (f) are for Samples (b) and (f), respectively, after reoxidation at 400°C.

Figure 5 shows that the reduction began at about 400°C, then stabilized quickly at a reduction corresponding to 1 *e*/mole (i.e., $Co^{3+} \rightarrow Co^{2+}$). At approximately 500°C, however, the reaction rate again increased and the reaction proceeded to almost exactly 3 *e*/mole (i.e., $Co^{3+} \rightarrow Co^{0}$). *Reduction to 1 e/mole* was very rapid, occurring in 30 min. at 400°C (Fig. 4). $LaCoO_3$, which is black in its oxidized state, turned to olive green (Co^{2+}) in this process. Patterns (a) and (b) of Fig. 6 show that the perovskite structure was slightly modified during this reduction. Even at room temperature in air, the reoxidation was fast; the olive green color changed to black instantaneously. Nevertheless, the total reoxidation was effected in O_2 at 400°C matching the data of Table 4, and then Pattern (c) was obtained. Note that Patterns (a) and (c) are virtually identical as expected. *Reduction to 3 e/mole* was reached in 4 h at 500°C (Fig. 4). The X-ray pattern (Fig. 6e) was now completely changed. It matched that of pure La_2O_3; all the peak indices correspond exactly to this structure. This was confirmed by the fact that the pattern changed very rapidly in air at room temperature to that of $La(OH)_3$. This chemistry is as expected if Co^0 is produced. The lines for this metal did not appear in Pattern (e). When, however, this material was heated in He for 5 h at 800°C, the expected lines appeared (Fig. 6g, compared with 6e). Interestingly, when air was replaced by pure O_2, Sample (e) became pyrophoric; it glowed. The X-ray pattern (not shown) then showed a substantial amount of Co_3O_4 plus La_2O_3 and perovskite. Nevertheless, it was possible to carry out the reoxidation slowly by using a mixture of 20% oxygen in helium; the reoxidation rate at 400°C is shown in Fig. 4. Moreover, the reoxidation under these conditions restored the perovskite structure (Fig. 6f). A comparison of Figs. 6a and f suggests that the chief difference is that the latter is more poorly crystallized than the former. Note that planes (104) and (110) have not been well resolved in Fig. 6f. These data, together with those of Table 4, show that these reactions are reversible under the conditions given. However, when the reduced Co was sintered (Sample g), reoxidation under the same conditions

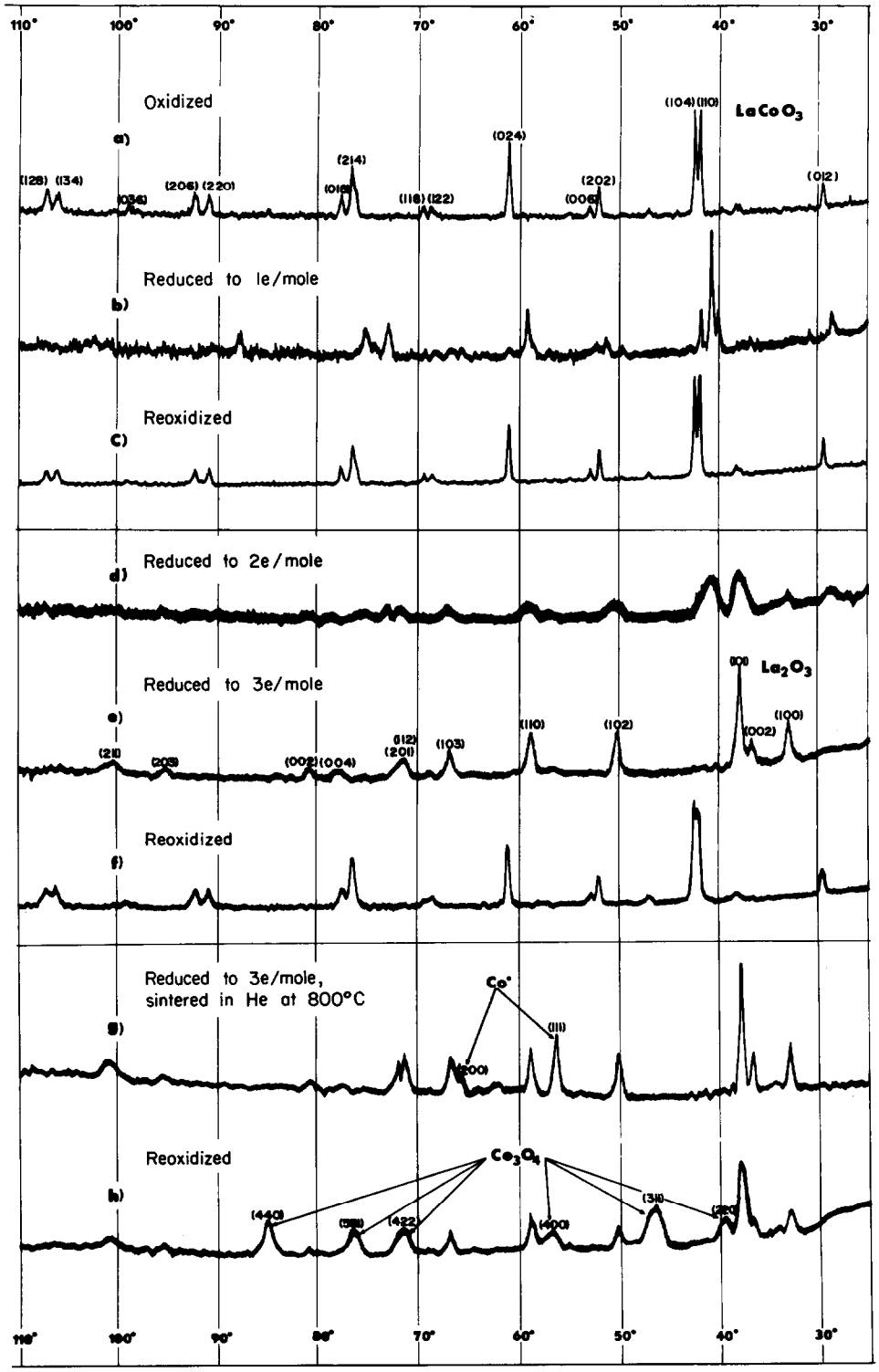

FIG. 6. X-Ray patterns of $LaCoO_3$ preparation taken at the labeled points on Fig. 5. (The rhombohedral structures of $LaCoO_3$ and La_2O_3 are indexed with hexagonal cells.)

did not produce a perovskite phase. Instead Co_3O_4 appeared (Fig. 6h).

Reduction to 2 e/mole led to a poorly resolved X-ray pattern (Fig. 6d) which may be interpreted as a mixture of phases. One of these was undoubtedly the residual $LaCoO_{2.5}$ and the other was poorly crystalline La_2O_3. This was confirmed by experiments in which the reduction was terminated at e/mole = 1.25 and 0.75, respectively. The new phase of La_2O_3 was already evident in the pattern from the former while that of the latter showed the beginning of the reconversion from the $LaCoO_{2.5}$ to the $LaCoO_3$ phase. The intensities of the lines around $2\theta = 40°$ correlated inversely with the extent of reduction. Reoxidation of the sample (20% O_2 in He, 400°C) yielded a pattern virtually identical to the X-ray pattern shown in Fig. 6f. The surface area of the starting structure, 16 m^2/g, decreased to 13 m^2/g for a reduction corresponding to 1 e/mole, and then was stable even up to a reduction of 3 e/mole. Repeated reductions and reoxidations did not further change at this value.

DISCUSSION

Bulk Properties

Ideally, perovskites have a cubic structure (Fig. 1), where each of the transition metal (B) ions is octahedrally coordinated by oxygen ions and the larger A ions are coordinated by 12 oxygens which in turn belong to eight BO_6 octahedra sharing corners. Actually most perovskites are not exactly cubic. For example, among the perovskites of interest here, $BaTiO_3$ is cubic above about 120°C, but below this critical temperature it undergoes a first-order transition and becomes ferroelectric. This transition is accompanied by a tetragonal distortion with $a = b = 3.994$ and $c = 4.038$ Å. This small change in edge length is sufficient, however, to effect a large change in catalytic properties (*9*). $SrTiO_3$, on the other hand, remains cubic with $a = b = c = 3.903$ Å (*25*). These two materials are classed as wide gap semiconductors (~3.2eV). The $LaCoO_3$ structure (*24*) has a rhombohedral distortion; its constants are $a = b = c = 3.82$ Å with $\alpha = \beta = \gamma = 90°, 70'$. It is classed as a "hopping" semiconductor with localized d electrons and a small energy barrier (~0.1 eV) for conduction. These small differences are reflected in the X-ray patterns of Fig. 2. Note that these patterns closely resemble each other, especially if small translational adjustments are made along the 2θ axis and one ignores intensity changes which reflect the different scattering cross section of the different ions. These patterns are in excellent agreement with literature data (*26*).

Surface Properties

The excellent crystallinity of these compounds, as seen by the symmetry and sharpness of the X-ray patterns and by the fact that the surface area remains constant even after the disappearance of the X-ray perovskite structure and its regeneration (Fig. 6), suggests that the surface areas of these perovskites consist of the surface exposed by the nonporous crystals constituting the sample. Given this condition, the maximum (theoretical) number of hydroxyl groups on a surface can be calculated by averaging values for the (100), (110), and (111) planes according to the Haüy law (*27*), which assumes that OH groups are required to terminate the lattice at each point where the surface atoms would otherwise be bound to atoms in the next higher layer, were it present. The results presented in Table 3 are sufficient to show that the surface actually covered by OH at 25°C is in substantial agreement with this expectation. At 600°C, on the other hand, the surfaces of the three perovskites were nearly completely dehydroxylated. This behavior resembles that of alumina and is typical for such oxides.

Reduction of perovskites

Given the surface areas of the perovskites, it was possible to estimate the ex-

tent of the reduction of the surface. For example, $SrTiO_3$, which had the greatest surface area of the three samples, was reduced in H_2 at 700°C to about 0.02 e/mole in 1 h. The color obtained after this reduction was blue, indicating the presence of Ti^{3+}. If it is assumed that the reduction corresponds to

$$2(O—\underset{|}{\overset{OH}{Ti^{4+}}}) + H_2 \xrightarrow{700°C} O—Ti^{3+}—O—Ti^{3+}—O + 2H_2O$$

and that at 700°C, only this surface reaction occurs, the overall extent of reduction (0.02 e/mole) corresponds to just about 1 e per surface Ti as represented above. Evidently, a large difference in reduction temperature is necessary for reduction of the surface and reduction of the bulk, i.e., 700 and 1200°C, respectively. This can easily be explained by the action of two totally different phenomena: (1) *surface reduction* at low temperature in which only the surface oxygens are removed and (2) *bulk reduction* at high temperature, which may require diffusion of the B cations through the matrix. Thus, with $LaCoO_3$, La_2O_3 was formed as all of the Co ions diffused out of the bulk as they were reduced by removal of oxygen at the surface. They must be expelled as the Co^0 atoms formed are much too large to remain in the lattice. Consequently, the reoxidation step may be quite sluggish because, as in the initial preparation, the two oxide phases must diffuse into each other.

With $BaTiO_3$, the consumption of H_2 at 700°C was too small to measure but the sample nevertheless turned blue, reflecting the behavior of $SrTiO_3$. The important point is, that for catalytic activity for redox reactions, only oxidation–reduction of the surface layer is required. This can occur without cation migration. The latter phenomena need only occur when bulk reduction of the lattice occurs.

The sites produced as the surface hydroxyls are removed by thermal dehydroxylation (Table 3) should be highly strained. As with other oxides sytems such coordinatively unsaturated sites (CUS) should be important for catalysis, e.g., in reactions involving H_2 (*28, 29*).

The results given in Table 4 suggest a general behavior for perovskites during reduction–reoxidation. These data show that the hydrogen consumed is about equal to the water produced (mainly in the reduction step) and twice the oxygen consumed in the reoxidation step. The overall reaction is

$$H_2 + \tfrac{1}{2} O_2 = H_2O.$$

If this can occur in two steps, it can occur in one, so that the perovskite is a redox catalyst. Evidently these materials do not retain much hydrogen during reduction.

In Table 4, the amount of water was always slightly less than expected, possibly because of adsorption on the glass walls of the apparatus; also, the amount of oxygen was slightly larger because of a small amount of vacuum reduction of the sample prior to adding the H_2. For example, evacuation of $SrTiO_3$ at 700°C changed its color to blue.

Table 4 and Fig. 6 are sufficient to write the following chemistry for $LaCoO_3$:

---

1 e/mole: $2LaCoO_3 + H_2 \xrightarrow{400°C} 2LaCoO_{2.5} + H_2O$ ($Co^{3+} \rightarrow Co^{2+}$),

2 e/mole: $2LaCoO_3 + 2H_2 \xrightarrow{500°C} LaCoO_{2.5} + 1/2La_2O_3 + Co^0 + 2H_2O$,

3 e/mole: $2LaCoO_3 + 3H_2 \xrightarrow{500°C} + La_2O_3 + 2Co^0 + 3H_2O$.

In these reactions, only cobalt, or element B of the perovskite, was reduced. Knowing that Ti^{3+} is blue, the same would seem to be true for $BaTiO_3$ and $SrTiO_3$ also, but only on the surface or at much higher temperatures. The surfaces of these materials did

not turn uniformly blue at 400°C, although some crystals showed this color. Bulk reduction (to 0.4 e/mole) was even more difficult. These data would suggest that $LaCoO_3$ should be a much better catalyst for the oxidation of CO than $BaTiO_3$. This is the result reported by Voorhoeve, *et al.* (*15*).

The reduction of Co^{3+} to Co^{2+}, as written above, was accompanied by a modification of the lattice; reoxidation reversed the process (Figs. 6a and b). It is interesting to note that the entire oxide lattice may play a role in catalysis here, as with bismuth molybdate systems.

The cobalt metal produced on the disappearance of the perovskite structure (reduction to 3 e/mole) exhibited extraordinary behavior. It was so finely dispersed in the resulting matrix of La_2O_3 that it did not produce coherent X-ray diffraction (Fig. 6e). Moreover, this Co^0 reacted very violently with oxygen at room temperature. This demonstrated that the surface area of the metal component was very high, i.e., the metal was highly dispersed.

At 800°C, the Co clustered in a He atmosphere (Figs. 6g and h) and restoration of the perovskite structure became very sluggish. These observations suggest that some perovskites may be used to prepare supported metal catalysts having highly dispersed B metal. It may be even more interesting as a dispersive agent since changes in the matrix may be effected by simple variation of the A component.

It is tempting to generalize the results reported herein to other perovskite systems. If this is done, some insight into the effectiveness of various perovskites as catalysts may be obtained, based on well-known chemical properties rather than solid-state physics. The two approaches should be complementary, however, and it is hoped that future work with these model systems will lead to a deeper understanding of the complex problems of catalysis.

A referee called our attention to a paper by Sis *et al.* (*30*) in which the structure and properties of $LaCoO_3$ were studied as the catalyst was reduced to $LaCoO_{2.5}$ by thermogravimetric and calorimetric techniques, by X-ray diffraction, and by magnetic property measurements. Where the data overlap ours the agreement is satisfactory and the conclusions drawn by these authors were in general concurrence with ours. However, they indexed their patterns on a monoclinic, rather than rhombohedral, lattice.

ACKNOWLEDGMENTS

It is a pleasure to acknowledge the support of this research by the National Science Foundation (Grant 0IP75-21230). In addition, one of us (MC) is grateful to the Centre National de la Recherche Scientifique for a leave of absence to carry out this research. Our thanks are also due Professor B. E. Brown for allowing us to use his X-ray diffractometer.

REFERENCES

1. Voorhoeve, R. J. H., "Advanced Materials in Catalysis," Chap. 5 (J. J. Burton and R. L. Garten, Eds.), Materials Science Series, Academic Press, New York, 1977.
2. Goodenough, J. B., *in* "Solid State Chemistry" (C. N. R. Rao, Ed.), pp. 215–364. Dekker, New York, 1974.
3. Goodenough, J. B., and Longo, J. M., *in* "Landolt–Börnstein New Series," Vol. 4, Part a, pp. 126–314. Springer-Verlag, Berlin, 1970.
4. Voorhoeve, R. J. H., *Science* **195,** 827 (1977).
5. Voorhoeve, R. J. H., Remeika, J. P., and Trinble, L. E., *Ann. N.Y. Acad. Sci.* **272,** 3 (1976).
6. Formenti, M., and Teichner, S. J., *Specialist Periodical Rep. Catal.* **2,** 87 (1979).
7. Wrighton, M. S., Wolczanski, P. T., and Ellis, A. B., *J. Solid State Chem.* **22,** 17 (1977); Wrighton, M. S., Ginley, D. S., Wolczanski, P. T., Ellis, A. B., Morse, D. L., and Linz, A., *Proc. Nat. Acad. Sci. USA* **72,** 1518 (1975); *J. Amer. Chem. Soc.* **98,** 2774 (1976).
8. Heminger, J. C., Lo, W. J., and Samorjai, G. A., *Chem. Phys. Lett.* **57,** 100 (1978).
9. Van Damme, H., and Hall, W. K., *J. Catal.* **69,** 371 (1981).
10. Kittel, C., "Introduction to Solid State Physics," 5th ed., Chap. 13, pp. 399 ff. Wiley, New York, 1976.
11. Wolfram, T., Krant, E. A., and Morin, F. J., *Phys. Rev. B* **7,** 1677 (1973).
12. Wolfram, T., and Morin, F. J., *Appl. Phys.* **8,** 125 (1975); *Phys. Rev. Lett.* **30,** 1214 (1973); *Phys. Rev. Lett.* **29,** 1383 (1972).

13. Paravanno, G., *J. Chem. Phys.* **20,** 342 (1952); *J. Amer. Chem. Soc.* **75,** 1448, 1497 (1953).
14. Kawai, T., Kinimori, K., Kondow, T., Onishi, T., and Tamaru, K., *Z. Phys. Chem. (Frankfurt)* **86,** 268 (1973).
15. Voorhoeve, R. J. H., Remeika, J. P., and Johnson, D. W., *Science* **177,** 353 (1972); **180,** 62 (1973).
16. Shizasake, S., Takahashi, K., and Yamamura, D. H., Kakegawa, K., and Mazi, *J. Solid State Chem.* **12,** 84 (1975).
17. Czoat, J. J., Tibbetts, G. G., and Katz, S., Symposium on Emission Control Catalyst, Amer. Chem. Soc., San Francisco, 1976; *Science* **194** (1976).
18. Johnson, D. W., Gallanger, P. K., Westheim, G. K., and Vogel, E. M., *J. Catal.* **48,** 87 (1977).
19. Baxter, G. P., and Fertig, G. J., *J. Amer. Chem. Soc.* **45,** 1228 (1923); Baxter, G. P., and Butler, A. Q., *J. Amer. Chem. Soc.* **48,** 3117 (1926); "G. Brauer's Handbuch des anorganischen preparation chemie," 2nd ed., 1045–1048 Stuttgart, 1963.
20. Brunauer, S., "The Adsorption of Gases and Vapors." Princeton Univ. Press, Princeton, N.J., 1943.
21. Hall, W. K., Cheselske, F. J., and Wallace, W. E., *J. Phys. Chem.* **63,** 505 (1959); *J. Phys. Chem.* **65,** 128 (1961).
22. Hall, W. K., Leftin, H. P., Cheselske, F. J., O'Reilly, D. E., *J. Catal.* **2,** 506 (1963).
23. Hall, W. K., Millman, W. S., Crespin, M., Cirillo, Jr., A. C., Abdo, S., *J. Catal.* **60,** 404 (1979).
24. Wold, A., Post, B., and Banks, E., *J. Amer. Chem. Soc.* **79,** 6365 (1957).
25. NBS Circular 539, Vol III, 1953.
26. National Bureau of Standards Monogr. 25, Sect. 9, 1971.
27. Bloss, D. F., "Crystallography and Crystal Chemistry." Holt, Rinehart & Winston, New York, 1971.
28. Burwell, R. L., Jr., and Stec, K. S., *J. Colloid Interface Sci.* **58,** 54 (1977).
29. Wolfram, T., and Morin, F. J., *Appl. Phys.* **8,** 125 (1975).
30. Sis, L. B., Wirtz, G. P., and Sorenson, S. C., *J. Appl. Phys.* **44,** 5553 (1973).